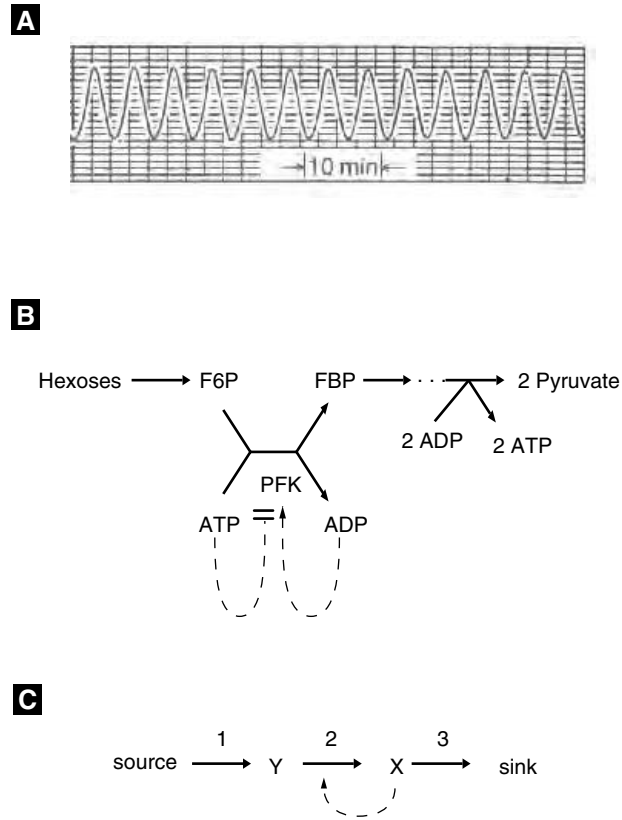


## Biochemical Oscillations

### John J. Tyson

Biochemical and biophysical rhythms are ubiquitous characteristics of living organisms, from rapid oscillations of membrane potential in nerve cells to slow cycles of ovulation in mammals. One of the first biochemical oscillations to be discovered was the periodic conversion of sugar to alcohol (“glycolysis”) in anaerobic yeast cultures (Chance et al. 1973). The oscillation can be observed as periodic changes in fluorescence from an essential intermediate, NADH; see Figure 9.1. In the laboratories of Britton Chance and Benno Hess, these oscillations were shown to arise from a curious property of the enzyme phosphofructokinase (PFK), which catalyzes the phosphorylation of fructose-6-phosphate to fructose-1,6-bisphosphate using ATP as the phosphate donor; Figure 9.1B. Although PFK consumes ATP, the glycolytic pathway produces more ATP than it consumes. To properly regulate ATP production, ATP inhibits PFK and ADP activates PFK. Hence, if the cell is energy “rich” (ATP high, ADP low), then PFK activity is inhibited, and the flux of sugars into the glycolytic pathway is shut down. As ATP level drops and ADP level increases, PFK is activated and glycolysis recommences. In principle, this negative feedback loop should stabilize the energy supply of the cell. However, because ATP is both a substrate of PFK and an inhibitor of the enzyme (likewise, ADP is both a product of PFK and an activator of the enzyme), the steady-state flux through the glycolytic pathway can be unstable, as we shall see, and the regulatory system generates sustained oscillations in all intermediates of the pathway.



**Figure 9.1** (A) Sustained oscillations in NADH fluorescence in yeast cells *Saccharomyces cerevisiae*. Reprinted from Pye (1971). (B) The control properties of the enzyme phosphofructokinase (PFK) are thought to be responsible for the generation of oscillations in the glycolytic pathway. PFK catalyzes the conversion of fructose-6-phosphate (F6P) into fructose-1,6-bisphosphate (FBP), using ATP as phosphate-group donor. PFK activity is allosterically modulated by ATP (inhibitor) and ADP (activator). F6P is steadily supplied to PFK by a sugar source ("Hexoses") and FBP is steadily utilized in the production of metabolites ("Pyruvate"). ADP and ATP are also recycled by other metabolic processes. (C) Simplified mechanism. Reaction 1 is a steady supply of substrate Y for reaction 2, whose product X is removed by reaction 3. X activates the enzyme (PFK) catalyzing reaction 2. Roughly speaking, Y = F6P + ATP, X = FBP + ADP, "source" = hexoses, and "sink" = pyruvate.

Another classic example of rhythmic behavior in biology is periodic growth and division of well-nourished cells. This phenomenon will be studied thoroughly in the next chapter, but for now, to illustrate some basic ideas, we focus on the periodic accumulation and degradation of cyclins during the division cycle of yeast cells; Figure 9.2. Kim Nasmyth and others have shown that these oscillations are intimately connected to dynamical interactions between CLN-type cyclins and CLB-type cyclins; Figure 9.2 (Nasmyth 1996). CLNs (in combination with a kinase subunit called CDC28) activate their own synthesis (product activation or "autocatalysis") and inhibit the degradation of CLBs. As CLBs accumulate, they inhibit the synthesis of CLNs, causing CLN-dependent kinase activity to drop and CLB degradation to increase. The mutual interplay of CLN and CLB generate the periodic appearance of their associated kinase activities, which drive the crucial events of the budding yeast cell cycle (bud emergence, DNA synthesis, mitosis, and cell division).

The third example that we shall use in this chapter concerns periodic changes in physiological properties (physical activity, body temperature, reproduction, etc.) entrained to the 24 h cycle of light and darkness so prevalent to life on earth. These rhythms are not driven solely by the external timekeeper, because they persist under

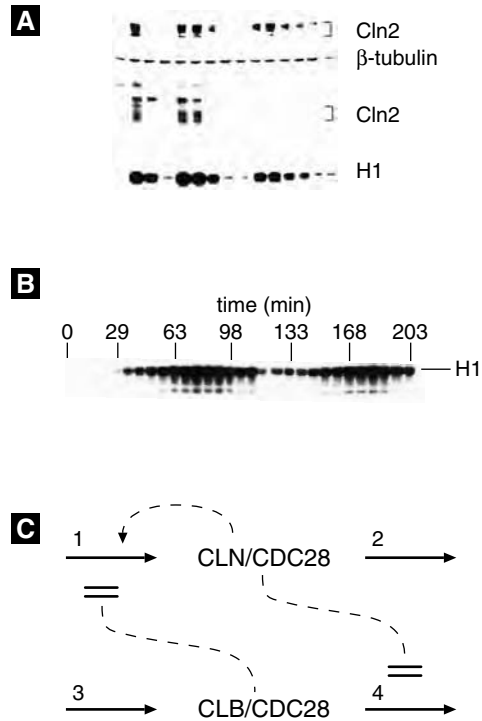


**Figure 9.2** Cyclin fluctuations during the cell cycle in budding yeast. (A) Samples are taken at increasing time points (left to right) from a synchronous culture of budding yeast cells and analyzed for CLN2/CDC28 protein content (top row) and CLN2/CDC28 kinase activity (last row, labeled “H1”). Reprinted from Tyers et al. (1993).  $\beta$ -tubulin serves as a control, nonoscillating, protein. (B) In a similar experiment, a synchronous culture of yeast cells is analyzed for CLB2/CDC28 activity (labeled “H1”; each column represents a 7 min increment). Reprinted from Surana et al. (1991). (C) Mechanism of cyclin oscillations. Budding yeast cells contain two classes of cyclins: CLN and CLB. These cyclins combine with a kinase partner (CDC28) to make active dimers. CDC28 subunits are always in excess, so dimer activity is limited by cyclin availability (i.e., cyclin synthesis and degradation, arrows 1-4 in the diagram). CLN/CDC28 activates the transcription factor that promotes CLN synthesis and inhibits the proteolytic enzymes that degrade CLB. In return, CLB/CDC28 inhibits the transcription factor that promotes CLN synthesis.

constant conditions of illumination and temperature; Figure 9.3A. Under constant conditions, the organism exhibits its own “endogenous” rhythm, which is close to, but not exactly, 24 h (hence “circadian,” or “nearly daily”). The basic molecular mechanism of circadian rhythms has been uncovered only recently, by research in the laboratories of Michael Rosbash, Michael Young, Jay Dunlap, and others (Dunlap 1999). Central to the mechanism is a protein called PER, which, after being synthesized in the cytoplasm, moves into the nucleus to inhibit the transcription of its own mRNA; Figure 9.3B. Hence, the regulatory mechanism for PER synthesis contains a time-delayed negative-feedback loop (Figure 9.3C), which, as we shall see, is another common theme in biochemical oscillators.

## 9.1 Biochemical Kinetics and Feedback

In general, a biochemical reaction network is a schematic diagram of “boxes and arrows.” Each box is a chemical species. Solid arrows represent chemical reactions producing or consuming a molecule. Dashed arrows represent control of a chemical reaction rate by a species that may not be a reactant or product of the reaction. Regulatory signals may be activatory (barbed end) or inhibitory (blunt end).

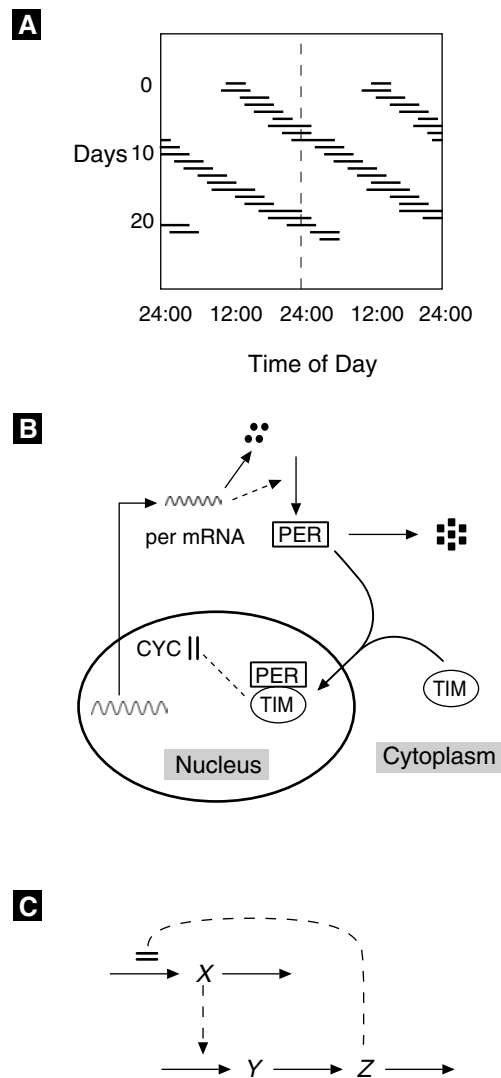


**Figure 9.3** (A) Endogenous circadian rhythm of activity. The black bars represent the sleep episodes of a human being isolated from all external temporal cues (variable light, temperature, etc.). The sleep episodes are plotted twice on each line to emphasize that the endogenous period of sleepiness is longer than 24 h. Data redrawn from Siffre (1975). (B) A protein called PER is known to play a crucial role in circadian rhythms in fruit flies and mice. The *per* gene is transcribed in the nucleus, with the help of two transcription factors, CLK and CYC. Then *per* mRNA is transported to the cytoplasm, where it codes for PER protein. PER protein is processed in the cytoplasm by phosphorylation and by binding to other proteins, such as TIM and CRY. Properly processed PER then moves into the nucleus, where it disrupts the binding of CLK and CYC, turning off the transcription of *per*. (C) A schematic representation of the negative-feedback loop in panel (B). This is **Goodwin's classical mechanism** for periodic protein expression, driven by feedback repression of transcription (Goodwin 1965).

To each reaction in a biochemical network is associated a rate law (with accompanying kinetic parameters). Hence, the network implies a set of rate equations of the form

$$\frac{dx}{dt} = v_{\text{in}1} + v_{\text{in}2} + \cdots - v_{\text{out}1} - v_{\text{out}2} - \cdots = f(x; p), \quad (9.1)$$

where  $t$  = time,  $x$  = concentration of species X, and  $v_{\text{in}1}, v_{\text{out}1}, \dots$  are the rates of the various reactions that produce and consume X. We lump together all these rate laws into a nonlinear function  $f(x; p)$ , where  $p$  is a vector of kinetic parameters. In general, we can think of  $x$  as a vector of concentrations of all the time-varying components in

**Table 9.1 Biochemical and Cellular Rhythms** Sources: Goldbeter (1996), Rapp (1979).

Rhythm	Period
Membrane potential oscillations	10 ms–10 s
Cardiac rhythms	1 s
Smooth muscle contraction	seconds – hours
Calcium oscillations	seconds–minutes
Protoplasmic streaming	1 min
Glycolytic oscillations	1 min–1 h
cAMP oscillations	10 min
Insulin secretion (pancreas)	minutes
Gonadotropic hormone secretion	hours
Cell cycle	30 min–24 h
Circadian rhythms	24 h
Ovarian cycle	weeks–months

the reaction network,  $x_i = [X_i]$ , and  $f$  as a vector-valued function. In component form,

$$\frac{dx_i}{dt} = f_i(x_1, x_2, \dots, x_n; p_1, p_2, \dots, p_r), \quad i = 1, \dots, n. \quad (9.2)$$

A “steady-state” solution  $(x_1^*, x_2^*, \dots, x_n^*)$  of the kinetic equations satisfies the algebraic equations

$$f_i(x_1, x_2, \dots, x_n; p_1, p_2, \dots, p_r) = 0, \quad i = 1, \dots, n. \quad (9.3)$$

Notice that steady-state concentrations depend on the parameter values  $x_i^* = x_i^*(p_1, \dots, p_r)$ . Moreover, the algebraic equations are generally nonlinear, so there may be multiple steady-state solutions. Of course, since we are dealing with chemical reaction systems, we are interested only in solutions that satisfy  $x_i \geq 0$  for all  $i$ .

In the theory of biochemical oscillations, based on rate equations of this sort, a crucial role is played by elements of the Jacobian matrix  $\mathbf{J} = [a_{ij}]$ , where  $a_{ij} = \partial f_i / \partial x_j$  evaluated at a steady-state solution. The matrix  $\mathbf{J}$  is a square matrix ( $n \times n$ ) dependent on parameter values and the steady state under consideration. The diagonal elements of the Jacobian matrix of a chemical reaction system are usually negative,  $a_{ii} < 0$ , because  $v_{\text{out}}$  terms in (9.1) are always proportional to the concentration of the substance being destroyed, so  $\partial f_i / \partial x_i$  always has one or more negative terms. Positive contributions to  $a_{ii}$  are rare because autocatalysis (reactions that produce  $X_i$  at a rate that increases with  $[X_i]$ ) is rare.

Common to biochemical networks are complex feedback loops, whereby the products of one reaction affect the rates of other reactions. A steady-state feedback loop can be defined as a set of nonzero elements of the Jacobian matrix that connect in a loop:  $a_{ij}a_{jk}a_{kl} \cdots a_{mi} \neq 0$ .

Representative feedback loops are illustrated in Figure 9.4.

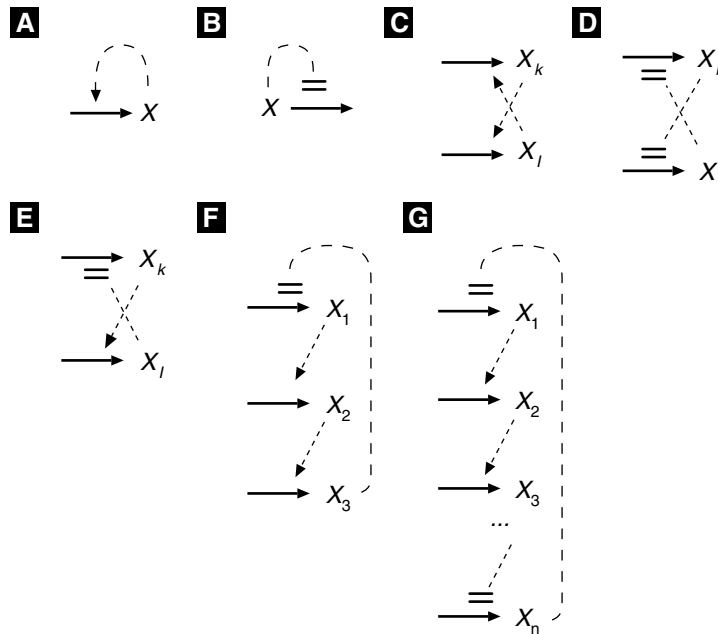


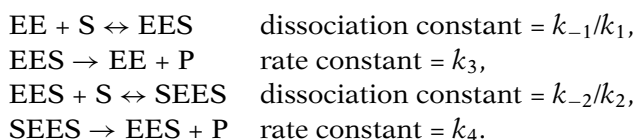
**Figure 9.4** Representative feedback loops.

- (A) Autocatalysis ( $a_{ii} > 0$ ), though rare, plays a major role in biochemical oscillations, as will become clear. We have already seen examples of autocatalysis in the mechanisms of glycolysis and yeast division; Figure 9.1 and Figure 9.2.
- (B) Autocatalysis also occurs when a chemical decelerates the rate of its own destruction.
- (C) Indirect autocatalysis occurs through a positive feedback loop ( $a_{ij}$  and  $a_{ji} > 0$ ), whereby  $X_i$  activates the production of  $X_j$ , and  $X_j$  returns the favor.
- (D) A two-component positive-feedback loop is also created by a pair of antagonistic species ( $a_{ij} < 0$  and  $a_{ji} < 0$ ).
- (E) A two-component negative-feedback loop ( $a_{ij}a_{ji} < 0$ ) is created when  $X_i$  activates the production of  $X_j$ , and  $X_j$  inhibits the production of  $X_i$ .
- (F) Longer negative feedback loops are common.
- (G) Long feedback loops are either positive or negative, depending on the sign of the product  $a_{1n}a_{n,n-1} \cdots a_{43}a_{32}a_{21}$ .

Before we can speak definitively about the effects of feedback in biochemical reaction networks, we need to know how to characterize the rates of enzyme-catalyzed reactions that are subject to regulation by “distant” effectors, i.e., chemical species other than the reactants and products of the enzyme.

## 9.2 Regulatory Enzymes

Regulatory enzymes are usually multisubunit proteins with binding sites for reactants and products (on the catalytic subunits) and for activators and inhibitors (on the regulatory subunits). Although there are more sophisticated and accurate ways to characterize the binding of small molecules to multisubunit proteins, we shall limit ourselves to a straightforward generalization of the Michaelis–Menten equation from Section 4.7. For simplicity, consider a two-subunit enzyme (EE) that converts substrate (S) into product (P). The binding constant and turnover number of each subunit depend on whether the other (identical) subunit is bound to S or not. The mechanism can be written



As in Section 4.1, we can make rapid-equilibrium approximations on the enzyme–substrate complexes:

$$\begin{aligned} \frac{[\text{EES}]}{[\text{EE}]_{\text{T}}} &= \frac{[\text{S}]/K_{\text{m1}}}{1 + ([\text{S}]/K_{\text{m1}}) + ([\text{S}]^2/(K_{\text{m1}}K_{\text{m2}}))}, \\ \frac{[\text{SEES}]}{[\text{EE}]_{\text{T}}} &= \frac{[\text{S}]^2/K_{\text{m1}}K_{\text{m2}}}{1 + ([\text{S}]/K_{\text{m1}}) + ([\text{S}]^2/(K_{\text{m1}}K_{\text{m2}}))}, \end{aligned}$$

where  $[\text{EE}]_{\text{T}} = [\text{EE}] + [\text{EES}] + [\text{SEES}]$ ,  $K_{\text{m1}} = (k_{-1} + k_3)/k_1$ , and  $K_{\text{m2}} = (k_{-2} + k_4)/k_2$ . Here  $K_{\text{m1}}$  is the Michaelis constant for the interaction of the enzyme with the first substrate to bind;  $K_{\text{m1}}$  is inversely proportional to the affinity of the enzyme for the first substrate;  $K_{\text{m2}}$  is inversely proportional to the affinity of the enzyme for the second substrate to bind.

Now it is easy to write an equation for the rate of the reaction:

$$v = \frac{d[\text{P}]}{dt} = -\frac{d[\text{S}]}{dt} = \frac{[\text{EE}]_{\text{T}} \left( \frac{[\text{S}]}{K_{\text{m1}}} \right) \left( k_3 + k_4 \left( \frac{[\text{S}]}{K_{\text{m2}}} \right) \right)}{1 + \left( \frac{[\text{S}]}{K_{\text{m1}}} \right) + \left( \frac{[\text{S}]^2}{K_{\text{m1}}K_{\text{m2}}} \right)}. \quad (9.4)$$

We can distinguish two interesting limiting cases of (9.4).

*Hill equation:*  $K_{\text{m1}} \rightarrow \infty, K_{\text{m2}} \rightarrow 0$ , such that  $K_{\text{m1}}K_{\text{m2}} = K_{\text{m}}^2 = \text{constant}$ ,

$$v = \frac{V_{\text{max}}([\text{S}]/K_{\text{m}})^2}{1 + ([\text{S}]/K_{\text{m}})^2}, \quad V_{\text{max}} = k_4[\text{EE}]_{\text{T}}; \quad (9.5)$$

*Substrate inhibition:*  $k_3 \rightarrow \infty, K_{\text{m1}} \rightarrow \infty, K_{\text{m2}} \rightarrow 0$ , such that  $K_{\text{m1}}K_{\text{m2}} = K_{\text{m}}^2 = \text{constant}$ ,  $k_3K_{\text{m2}} \rightarrow \infty$ , and  $k_3[\text{EE}]_{\text{T}}K_{\text{m}}/K_{\text{m1}} = V_{\text{max}} = \text{constant}$ ,

$$v = \frac{V_{\text{max}}[\text{S}]/K_{\text{m}}}{1 + ([\text{S}]/K_{\text{m}})^2}. \quad (9.6)$$

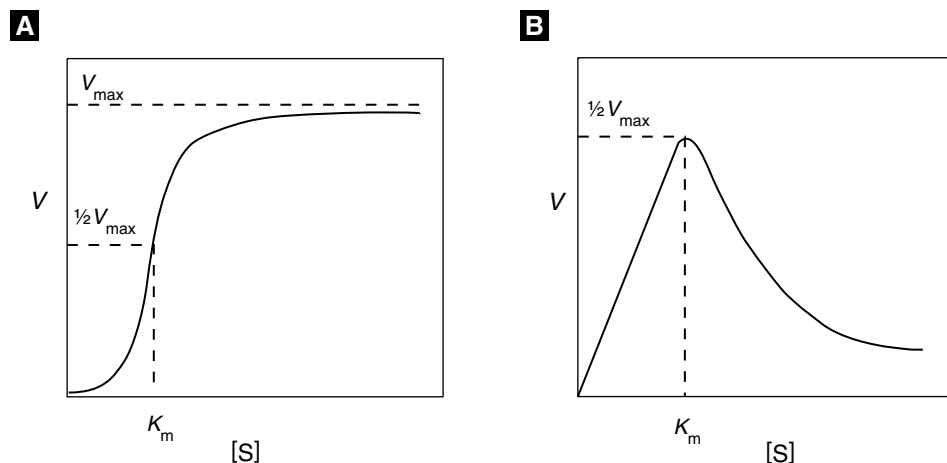


**Figure 9.5** Rate laws for activation and inhibition of multisubunit enzymes by cooperative binding.

Equations (9.5) and (9.6) are plotted in Figure 9.5.

Rate laws like (9.4) are said to express “cooperative” kinetics. The “empty” enzyme (EE) has low affinity for substrate ( $K_{m1}$  large), but as the enzyme picks up its first substrate molecule, the two subunits change their conformation to a high affinity form ( $K_{m2}$  small, such that  $K_m = (K_{m1}K_{m2})^{1/2}$  is physiologically significant).

If the subunits do not exhibit cooperative binding, then  $k_1 = 2k_2$ ,  $2k_{-1} = k_{-2}$ ,  $k_4 = 2k_3$ , and hence

$$v = \frac{V_{\max}[S]}{K_m + [S]}. \quad (9.7)$$

That is, we regain the Michaelis–Menten rate law, with  $V_{\max} = 2k_3$  and  $K_m = 2(k_{-1} + k_3)/k_1$ .

Cooperative binding of ligands to a multisubunit enzyme is not limited to substrates. Other small molecules may bind to the enzyme and alter its catalytic properties (either its affinity for substrates or its rate of converting bound substrates into products). Such enzymes are called “allosteric” because in addition to substrate-binding sites, they have “other sites” for binding regulatory molecules that either activate or inhibit the enzyme. Allosteric proteins play crucial roles in the regulation of metabolic pathways, membrane transport, gene expression, etc. Relatively simple algebraic expressions for allosteric effects can be derived by the reasoning behind (9.4).

For instance, consider a tetrameric enzyme, with two catalytic subunits (EE) and two regulatory subunits (RR), which bind substrate (S) and ligand (L), respectively. In this case, the holoenzyme may exist in nine different forms. If each association–dissociation reaction is in rapid equilibrium at given concentrations of substrate and



ligand, then

$$[E_T] = [EE_{00}] \left( 1 + \frac{[S]}{K_{m1}} + \frac{[S]^2}{K_{m1}K_{m2}} \right) \left( 1 + \frac{[L]}{K_{n1}} + \frac{[L]^2}{K_{n1}K_{n2}} \right)$$

where  $[E]_T$  = total concentration of enzyme in all nine forms,  $[EE_{00}]$  = concentration of holoenzyme unbound to substrate or ligand,  $[S]$  = substrate concentration,  $[L]$  = ligand concentration,  $K_m$ 's = Michaelis constants for substrate binding (e.g.,  $K_{m1} = k_{-1}/k_1$ ), and  $K_n$ 's = Michaelis constants for ligand binding (defined similarly). If, for example, the only form of the enzyme with significant catalytic activity is



then the rate of the reaction is

$$v = V_{\max} \frac{[S]^2/(K_{m1}K_{m2})}{1 + [S]/K_{m1} + [S]^2/(K_{m1}K_{m2})} \cdot \frac{[L]^2/(K_{n1}K_{n2})}{1 + [L]/K_{n1} + [L]^2/(K_{n1}K_{n2})}. \quad (9.8)$$

In this case, the ligand is an allosteric *activator* of the enzyme. For an allosteric *inhibitor*, the enzyme is most active when no ligand is bound to the regulatory subunits; hence

$$v = V_{\max} \frac{[S]^2/(K_{m1}K_{m2})}{1 + [S]/K_{m1} + [S]^2/(K_{m1}K_{m2})} \cdot \frac{1}{1 + [L]/K_{n1} + [L]^2/(K_{n1}K_{n2})}. \quad (9.9)$$

A comprehensive and accurate kinetic theory of allosteric enzymes (Rubinow 1980; Goldbeter 1996) is much more complicated than what has been presented, but (9.8) and (9.9) will serve our purposes in this chapter.

Finally, suppose EE and S above are not “multisubunit enzyme” and “substrate” but “dimeric transcription factor” and “ligand.” The active form of the transcription factor promotes the expression of some gene, and the presence of ligand alters the distribution of transcription factor among its various forms: EE, EES, and SEES. Depending on which form of transcription factor is most active, the rate of gene expression can be activated and/or inhibited by ligand:

ligand effect	active form	relative rate of gene expression
inhibition	EE	$\frac{1}{1 + ([S]/K_{m1}) + ([S]^2/K_{m1}K_{m2})}$ ,
activation	SEES	$\frac{[S]^2/K_{m1}K_{m2}}{1 + ([S]/K_{m1}) + ([S]^2/K_{m1}K_{m2})}$ ,
mixed	EES	$\frac{[S]/K_{m1}}{1 + ([S]/K_{m1}) + ([S]^2/K_{m1}K_{m2})}$ .

### 9.3 Two-Component Oscillators Based on Autocatalysis

First, we consider two minimal requirements for oscillations in chemical reaction systems.

1. If the “network” is absurdly simple, with only one time-varying component, then oscillations are, generally speaking, impossible. (Proof: For  $x(t)$  to be periodic,  $dx/dt$  must take on both positive and negative values at some values of  $x$ , which is impossible if  $f(x; p)$  is a continuous single-valued function of  $x$ .) Thus, to understand biochemical oscillations, we must start with two-component networks, described by a pair of ODEs

$$\begin{aligned}\frac{dx}{dt} &= f(x, y), \\ \frac{dy}{dt} &= g(x, y),\end{aligned}\tag{9.10}$$

where  $x$  and  $y$  are (nonnegative) concentrations of the two components, and we have suppressed the dependence of  $f$  and  $g$  on parameters, for the time being.

2. Bendixson’s negative criterion states that if  $\partial f/\partial x + \partial g/\partial y$  is of constant sign in some region  $R$  of the  $x, y$  plane, then there can be no periodic solution of system (9.10) in  $R$ . Since  $\partial f/\partial x$  and  $\partial g/\partial y$  are usually negative (refer to our earlier discussion of the Jacobian matrix), Bendixson’s criterion requires that a two-component chemical reaction system have an autocatalytic step ( $\partial f/\partial x > 0$  or  $\partial g/\partial y > 0$ ) in order to exhibit sustained oscillations.

In general, we can expect system (9.10) to have one or more steady-state solutions  $(x^*, y^*)$ , satisfying  $f(x^*, y^*) = 0$  and  $g(x^*, y^*) = 0$ . The stability of such steady states is determined by the eigenvalues of the Jacobian matrix evaluated at the steady state

$$\mathbf{J} = \begin{bmatrix} f_x(x^*, y^*) & f_y(x^*, y^*) \\ g_x(x^*, y^*) & g_y(x^*, y^*) \end{bmatrix} = \begin{bmatrix} a_{11} & a_{12} \\ a_{21} & a_{22} \end{bmatrix}.$$

The eigenvalues of  $\mathbf{J}$  are the roots of the characteristic equation  $\lambda^2 - (a_{11} + a_{22})\lambda + (a_{11}a_{22} - a_{12}a_{21}) = 0$ , namely,

$$\lambda_{\pm} = \frac{1}{2} \left[ a_{11} + a_{22} \pm \sqrt{(a_{11} + a_{22})^2 - 4(a_{11}a_{22} - a_{12}a_{21})} \right].$$

For the steady state to be stable,  $\text{Re}(\lambda)$  must be negative for both eigenvalues. If  $a_{11}a_{22} - a_{12}a_{21} = \det(\mathbf{J}) < 0$ , then  $\mathbf{J}$  has one positive and one negative eigenvalue, and the steady state is a saddle point. If  $\det(\mathbf{J}) > 0$  and  $a_{11} + a_{22} = \text{tr}(\mathbf{J}) < 0$ , then the steady state is stable, whereas, if  $\det(\mathbf{J}) > 0$  and  $\text{tr}(\mathbf{J}) > 0$ , then the steady state is an unstable node or focus.

In general, the trace and determinant of  $\mathbf{J}$  depend continuously on the kinetic parameters in  $f$  and  $g$ . If by varying one of these parameters (call it  $p_1$ ) we can carry  $\text{tr}(\mathbf{J})$  from negative to positive values, with  $\det(\mathbf{J}) > 0$ , then the steady state loses stability at

$\text{tr}(\mathbf{J}) = 0$  (when  $p_1 = p_{\text{crit}}$ , say). At the bifurcation point,  $\text{tr}(\mathbf{J}) = a_{11} + a_{22} = 0$ , the eigenvalues are pure imaginary numbers,  $\lambda_{\pm} = \pm i\omega$ ,  $\omega = \sqrt{(a_{11} + a_{22})^2 - 4(a_{11}a_{22} - a_{12}a_{21})}$ . Close to the bifurcation point, i.e.,  $p_1 \approx p_{\text{crit}}$ , small-amplitude limit-cycle solutions surround the steady state, and the period of oscillation is close to  $2\pi/\omega$ . We say that periodic solutions arise by a **Hopf bifurcation** at  $p_1 = p_{\text{crit}}$  (Section A.5.2).

Biochemical oscillations usually arise by this mechanism, so we will consider first the requirements for Hopf bifurcation in a two-component network. In chemical reaction systems the diagonal elements of the Jacobian matrix are usually negative numbers, reflecting the various steps by which species X is transformed into something else. If both  $a_{11}$  and  $a_{22}$  are always negative, then  $\text{tr}(\mathbf{J})$  never changes sign, and a Hopf bifurcation cannot occur. At least one of them must be positive for some values of the kinetic parameters. For a diagonal element to be positive, species X must be “autocatalytic;” i.e., with increasing [X], the rates of production of X increase faster than the rates of destruction. If  $a_{11}$  and  $a_{22}$  are of opposite sign, then  $a_{12}$  and  $a_{21}$  must also be of opposite sign in order for  $\det(\mathbf{J})$  to be positive. Thus we have two characteristic sign patterns for Jacobian matrices that typically produce Hopf bifurcations in chemical reaction systems with two time-dependent components:

$$\mathbf{J} = \begin{bmatrix} + & + \\ - & - \end{bmatrix} \text{ and } \mathbf{J} = \begin{bmatrix} + & - \\ + & - \end{bmatrix}. \quad (9.11)$$

Next, we describe the sorts of biochemical networks that produce these sign patterns and generate periodic solutions via Hopf bifurcations.

### 9.3.1 Substrate–Depletion Oscillator

The simplest oscillatory mechanism is probably the linear pathway in Figure 9.1C. Species Y is converted into X by an enzyme that is activated by its product. Hence, the production of X is autocatalytic; the reaction speeds up as [X] increases, until the substrate Y is depleted so much that the reaction ceases.

Using a rate law for the allosteric enzyme like those derived in Section 9.2, we can write a pair of ODEs describing this mechanism:

$$\begin{aligned} \frac{d[\text{X}]}{dt} &= v_2[\text{Y}] \frac{\epsilon^2 + ([\text{X}]/K_n)^2}{1 + ([\text{X}]/K_n)^2} - k_3[\text{X}], \\ \frac{d[\text{Y}]}{dt} &= k_1 - v_2[\text{Y}] \frac{\epsilon^2 + ([\text{X}]/K_n)^2}{1 + ([\text{X}]/K_n)^2}. \end{aligned} \quad (9.12)$$

The rational function

$$\frac{\epsilon^2 + ([\text{X}]/K_n)^2}{1 + ([\text{X}]/K_n)^2}$$

represents activation of the allosteric enzyme by binding of product X to the enzyme’s regulatory sites. The constant  $\epsilon^2$  is the activity of the enzyme with no product bound relative to its activity when its regulatory sites are saturated by product molecules. We

assume that product-binding to regulatory sites is highly cooperative, so that we can neglect the fraction of enzyme with only one product molecule bound. We shall also assume that  $\epsilon \ll 1$ .

It is convenient to define “dimensionless” variables  $x = [X]/K_n$ ,  $y = [Y]/K_n$ , and  $t' = k_3 t$ , and a new variable  $z = x + y$ , and write system (9.12) as

$$\begin{aligned}\frac{dx}{dt'} &= v(z-x) \frac{\epsilon^2 + x^2}{1+x^2} - x, \\ \frac{dz}{dt'} &= \kappa - x,\end{aligned}\tag{9.13}$$

where  $v = v_2/k_3$  and  $\kappa = k_1/(k_3 K_n)$ . The steady state for this model satisfies  $x^* = \kappa$  and  $v(z^* - \kappa) = \kappa(1 + \kappa^2)/(\epsilon^2 + \kappa^2)$ . For the Jacobian matrix of system (9.13) at the steady state, it is easy to show that  $\det(\mathbf{J}) = v(\epsilon^2 + \kappa^2)/(1 + \kappa^2) > 0$  and

$$\begin{aligned}\text{tr}(\mathbf{J}) &= -1 - v \frac{\epsilon^2 + \kappa^2}{1 + \kappa^2} + \frac{2\kappa^2(1 - \epsilon^2)}{(\epsilon^2 + \kappa^2)(1 + \kappa^2)} \\ &= -\frac{(1+v)\kappa^4 - (1-3\epsilon^2 - 2v\epsilon^2)\kappa^2 + \epsilon^2(1+v\epsilon^2)}{(\epsilon^2 + \kappa^2)(1 + \kappa^2)}.\end{aligned}\tag{9.14}$$

It should be obvious from (9.14) that  $\text{tr}(\mathbf{J}) < 0$  and the steady state is stable if  $\kappa$  is either close to 0 or very large. On the other hand,  $\text{tr}(\mathbf{J}) > 0$ , and the steady state is unstable if  $\kappa$  takes on intermediary values. For  $\epsilon$  small, the steady state is unstable when  $\kappa^2 - \epsilon^2 > 0$  and when  $-(1+v)\kappa^4 + \kappa^2 > 0$ , i.e., when

$$\epsilon < \kappa < (1-v)^{-1/2},\tag{9.15}$$

which may, alternatively, be expressed as conditions on the input rate of Y:

$$\epsilon < \frac{k_1}{k_3 K_n} < \sqrt{\frac{k_3}{k_3 + v_2}}.\tag{9.16}$$

Between these limits the system executes stable limit cycle oscillations.

As we have often seen in this book, for two-component dynamical systems it is informative to plot nullclines in the phase plane. For system (9.13),

$$\begin{aligned}x\text{-nullcline: } z &= x + \frac{x(1+x^2)}{v(\epsilon^2+x^2)}, \\ z\text{-nullcline: } x &= \kappa.\end{aligned}$$

These nullclines are plotted in Figure 9.6. The  $x$ -nullcline has extrema at the roots of

$$(1+v)x^4 - (1-3\epsilon^2 - 2v\epsilon^2)x^2 + \epsilon^2(1+v\epsilon^2) = 0.$$

Notice that the steady state loses stability exactly when the steady state passes through the extrema of the  $x$ -nullcline.

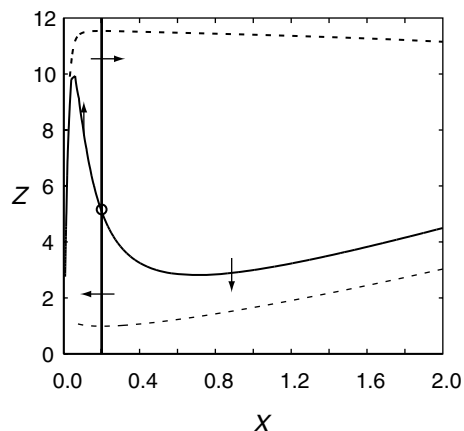


**Figure 9.6** Phase plane portrait of a typical substrate–depletion oscillator, (9.13). Parameter values:  $\nu = 1, \kappa = 0.2, \epsilon = 0.05$ . The solid lines are the  $x$ -nullcline (marked by short vertical arrows) and the  $y$ -nullcline (horizontal arrows). The nullclines intersect at an unstable steady state (o). The dashed line is the stable limit cycle solution (periodic orbit) of the dynamical system.

### 9.3.2 Activator–Inhibitor Oscillator

Looking back to (9.11), we see that there are two sign patterns consistent with Hopf bifurcation in a two-component biochemical reaction system. The first is illustrated by the substrate–depletion oscillator in Figure 9.1, and the second by the activator–inhibitor model in Figure 9.2. The ODEs describing Figure 9.2 are

$$\begin{aligned}\frac{d[X]}{dt} &= \nu_1 \frac{\epsilon^2 + ([X]/K_m)^2}{1 + ([X]/K_m)^2} \cdot \frac{1}{1 + ([Y]/K_n)} - k_2[X], \\ \frac{d[Y]}{dt} &= k_3 - \frac{k_4[Y]}{1 + ([X]/K_j)^2},\end{aligned}$$

where  $X = \text{CLN}/\text{CDC28}$  and  $Y = \text{CLB}/\text{CDC28}$ . In terms of dimensionless variables ( $x = [X]/K_m, y = [Y]/K_n, t' = \nu_1 t/K_m$ ), these equations become

$$\begin{aligned}\frac{dx}{dt'} &= \frac{\epsilon^2 + x^2}{1 + x^2} \cdot \frac{1}{1 + y} - ax, \\ \tau \frac{dy}{dt'} &= b - \frac{y}{1 + cx^2},\end{aligned}\tag{9.17}$$

where  $a = k_2 K_m / \nu_1, b = k_3 / (k_4 K_n), c = (K_m / K_j)^2$ , and  $\tau = \nu_1 / (k_4 K_m)$ .

Rather than analyze the stability of the steady state algebraically, which is difficult, we go directly to phase plane portraits of Figure 9.7. It is easy to find parameter values that produce either limit cycle oscillations or bistability.

Intuitively, the origin of the oscillations is clear. When  $Y$  is rare,  $X$  increases autocatalytically. Abundant  $X$  stimulates accumulation of  $Y$  (by inhibiting  $Y$ 's degradation), which feeds back to inhibit the production of  $X$ . After  $X$  disappears,  $Y$  is also destroyed, and then  $X$  can make a comeback. Mechanisms like this one, whose Jacobian matrix

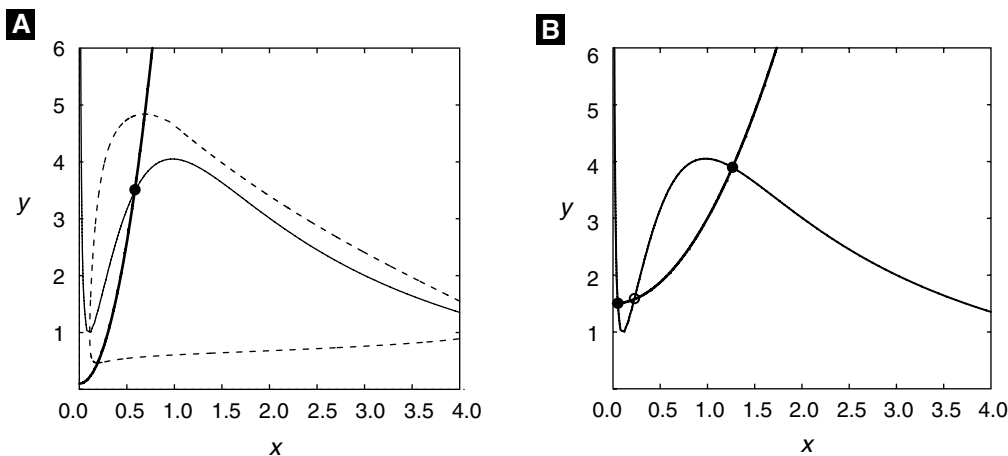


**Figure 9.7** Phase plane portrait of a typical activator–inhibitor system, (9.17). The solid lines are nullclines, intersecting at stable (●) or unstable (○) steady states. The dashed line is a closed orbit of the dynamical system. (A) Oscillation, for  $a = 0.1, b = 0.1, c = 100, \epsilon = 0.1, \tau = 5$ . (B) Bistability, for  $a = 0.1, b = 1.5, c = 1, \epsilon = 0.1, \tau = 5$ .

has sign pattern

$$\begin{bmatrix} + & - \\ + & - \end{bmatrix},$$

are called activator–inhibitor models.

Two-component mechanisms with autocatalysis easily generate oscillations and bistability, as we have just seen. They also exhibit a rich structure of bifurcations to more complicated behavior (Boissonade and De Kepper 1980; Guckenheimer 1986).

## 9.4 Three-Component Networks Without Autocatalysis

In the previous section we have seen that two-component reaction systems can oscillate if they have autocatalysis ( $a_{11}$  or  $a_{22}$  positive) and negative feedback ( $a_{12}$  and  $a_{21}$  opposite sign). In this section we examine networks of three components ( $x, y, z$ ) with Jacobian matrices of the form

$$\mathbf{J}_{\pm} = \begin{bmatrix} -\alpha & 0 & \pm\phi \\ c_1 & -\beta & 0 \\ 0 & c_2 & -\gamma \end{bmatrix},$$

where  $\alpha, \beta, \gamma, c_1, c_2, \phi$  are all positive constants. Since the diagonal elements of the Jacobian are all negative, the system lacks autocatalysis. The Jacobian  $\mathbf{J}_+$  describes a system with a positive feedback loop, and  $\mathbf{J}_-$  one with a negative feedback loop.

### 9.4.1 Positive Feedback Loop and the Routh–Hurwitz Theorem

First, let us see whether Hopf bifurcations are possible in a system with a pure positive-feedback loop, i.e., a Jacobian of the form  $\mathbf{J}_+$  at the steady state. Recall that the condition for a Hopf bifurcation is that the Jacobian matrix has a pair of purely imaginary eigenvalues  $\lambda_{\pm} = \pm i\omega$ . The eigenvalues of  $\mathbf{J}_+$  are roots of the characteristic equation

$$\begin{aligned} G(\lambda) &= \lambda^3 + (\alpha + \beta + \gamma)\lambda^2 + (\alpha\beta + \beta\gamma + \gamma\alpha)\lambda + \alpha\beta\gamma - c_1c_2\phi \\ &= \lambda^3 + A\lambda^2 + B\lambda + C \\ &= 0. \end{aligned}$$

The roots of this equation can be characterized by the Routh–Hurwitz theorem. Let  $G(\lambda_i) = 0$  for  $i = 1, 2, 3$ . Then  $\text{Re}(\lambda_i) < 0$  for  $i = 1, 2, 3$  if and only if (i)  $A > 0$ , (ii)  $C > 0$ , and (iii)  $AB > C$ . (For a proof, see Gantmacher (1959), p. 190.) Hence, in order for the steady state of the positive feedback loop to be unstable, we must insist that  $C = \alpha\beta\gamma - c_1c_2\phi < 0$ . In this case,  $\mathbf{J}_+$  has at least one real positive root, call it  $\lambda_1 > 0$ . Then,  $G(\lambda) = (\lambda - \lambda_1)H(\lambda)$ , where  $H(\lambda) = \lambda^2 + D\lambda + E$  and  $D = A + \lambda_1 > 0$ ,  $E = -C/\lambda_1 > 0$ . From the quadratic formula, it follows that the two roots of  $H(\lambda) = 0$  must have  $\text{Re}(\lambda_i) < 0$ . Hence, it is impossible for a steady state with Jacobian matrix  $\mathbf{J}_+$  to undergo a Hopf bifurcation.

It is possible for a positive feedback loop to have multiple steady state solutions, with two stable nodes separated by a saddle point. At the saddle point,  $\lambda_1 > 0$  and  $\text{Re}(\lambda_i) < 0$  for  $i = 2, 3$ . For an example, see Exercise 9.6.

### 9.4.2 Negative Feedback Oscillations

The Jacobian  $\mathbf{J}_-$  determines the stability of the steady state in a three-variable system with a pure negative feedback loop. In this case,

$$G(\lambda) = \lambda^3 + (\alpha + \beta + \gamma)\lambda^2 + (\alpha\beta + \beta\gamma + \gamma\alpha)\lambda + \alpha\beta\gamma + c_1c_2\phi = 0,$$

and the Routh–Hurwitz theorem implies that the steady state is unstable if and only if

$$(\alpha + \beta + \gamma)(\alpha\beta + \beta\gamma + \gamma\alpha) < \alpha\beta\gamma + c_1c_2\phi.$$

Furthermore, if equality holds, then  $G(\lambda) = (\lambda + A)(\lambda^2 + B)$ , so  $G(\lambda)$  has conjugate roots on the imaginary axis at  $\lambda = \pm i\sqrt{\alpha\beta + \beta\gamma + \gamma\alpha}$ .

### 9.4.3 The Goodwin Oscillator

The quintessential example of a biochemical oscillator based on negative feedback alone (Figure 9.3C) was invented by Brian Goodwin ((Goodwin 1965; Goodwin 1966); see also Griffith (1968a)). The kinetic equations describing this mechanism are

$$\frac{d[X_1]}{dt} = \frac{v_0}{1 + ([X_3]/K_m)^p} - k_1[X_1],$$

$$\begin{aligned}\frac{d[X_2]}{dt} &= v_1[X_1] - k_2[X_2], \\ \frac{d[X_3]}{dt} &= v_2[X_2] - k_3[X_3].\end{aligned}$$

Here  $[X_1]$ ,  $[X_2]$ , and  $[X_3]$  are concentrations of mRNA, protein, and end product, respectively;  $v_0$ ,  $v_1$ , and  $v_2$  determine the rates of transcription, translation, and catalysis;  $k_1$ ,  $k_2$ , and  $k_3$  are rate constants for degradation of each component;  $1/K_m$  is the binding constant of end product to transcription factor; and  $p$  is a measure of the cooperativity of end product repression.

Next we introduce dimensionless variables:

$$\begin{aligned}x_1 &= \frac{v_1 v_2 [X_1]}{k_2 k_3 K_m}, \\ x_2 &= \frac{v_2 [X_2]}{k_3 K_m}, \\ x_3 &= [X_3]/K_m, \\ t' &= \alpha t,\end{aligned}$$

where  $\alpha = (v_0 v_1 v_2)/(K_m k_2 k_3)$ .

In terms of these new variables, the dynamical system becomes

$$\begin{aligned}\frac{dx_1}{dt'} &= \frac{1}{1+x_3^p} - b_1 x_1, \\ \frac{dx_2}{dt'} &= b_2(x_1 - x_2), \\ \frac{dx_3}{dt'} &= b_3(x_2 - x_3),\end{aligned}$$

where  $b_i = k_i/\alpha$ .

Furthermore, to make the example easier, we shall assume that  $b_1 = b_2 = b_3$ . In this case, the dynamical system has a steady state at  $x_1 = x_2 = x_3 = \xi$ , where  $\xi$  is the unique real positive root of  $1/(1 + \xi^p) = b\xi$ . The Jacobian matrix at this steady state is  $\mathbf{J}_-$ , with  $\alpha = \beta = \gamma = b$ ,  $c_1 = c_2 = b$ , and  $\phi = (p\xi^{p-1})/(1 + \xi^p)^2 = bp(1 - b\xi) > 0$ . Hence, the characteristic equation is  $(b + \lambda)^3 + b^2\phi = 0$ , whose roots are

$$\begin{aligned}\lambda_1 &= -b - b\sqrt[3]{p(1 - b\xi)} < 0, \\ \lambda_{2,3} &= -b + b\sqrt[3]{p(1 - b\xi)} [\cos(\pi/3) \pm i \sin(\pi/3)].\end{aligned}$$

The steady state of Goodwin's model is unstable if  $\text{Re}(\lambda_{2,3}) > 0$ , i.e., if  $-b + (b/2)\sqrt[3]{p(1 - b\xi)} > 0$ . This condition is equivalent to  $p(1 - b\xi) > 8$ , or  $b\xi < (p - 8)/p$ . Hence, if  $p$  (the cooperativity of end product repression) is greater than 8, then we can choose  $k$  small enough to destabilize the steady-state solution of Goodwin's equations. At the critical value of  $k$ , when  $\text{Re}(\lambda_{2,3}) = 0$ , the steady state undergoes a



Hopf bifurcation, spinning off small-amplitude periodic solutions with period close to  $2\pi/\text{Im}(\lambda_{2,3}) = 2\pi/(b\sqrt{3})$ .

In Exercise 8 you are asked to generalize this derivation to negative feedback loops with an arbitrary number  $n$  of components. You will find that the steady state is unstable when  $b\xi < (p - p_{\min})/p$ , where  $p_{\min} = \sec^n(\pi/n)$ . Notice that  $p_{\min} \rightarrow 1^+$  as  $n \rightarrow \infty$ , i.e., the minimum cooperativity of endproduct repression required for oscillations becomes small as the length of the feedback loop increases.

The analysis of Hopf bifurcations in Goodwin's model uncovers a number of problems with his negative-feedback mechanism for biochemical oscillations (Griffith 1968a). In a three-variable system (mRNA, protein, end product), the cooperativity of feedback must be very high,  $p > 8$ . Also, it is necessary, in this case, for the degradation rate constants of the three components to be nearly equal. If not,  $p_{\min}$  increases dramatically; e.g., if one of the  $k_i$ 's is tenfold larger than the other two, then  $p_{\min} = 24$ . The value of  $p_{\min}$  can be reduced by lengthening the loop, but one must still ensure that the  $k_i$ 's are nearly equal.

Bliss, Painter and Marr (Bliss et al. 1982) fixed these problems by a slight modification of Goodwin's equations:

$$\begin{aligned}\frac{dx_1}{dt} &= \frac{a}{1+x_3} - b_1x_1, \\ \frac{dx_2}{dt} &= b_1x_1 - b_2x_2, \\ \frac{dx_3}{dt} &= b_2x_2 - \frac{cx_3}{K+x_3}.\end{aligned}$$

Notice that the feedback step is no longer cooperative ( $p = 1$ ), and the uptake of end product is now a Michaelis-Menten function. The steady state of this system is  $x_1^* = a/(b_1(1+\xi))$ ,  $x_2^* = a/(b_2(1+\xi))$ ,  $x_3^* = \xi$ , where  $\xi$  is the unique real positive root of  $a/(1+\xi) = c\xi/(K+\xi)$ . The stability of this steady state is determined by the roots of the characteristic equation  $(b_1 + \lambda)(b_2 + \lambda)(\beta + \lambda) + b_1b_2\phi = 0$ , where  $\beta = cK/(K+\xi)^2$  and  $\phi = a/(1+\xi)^2$ .

The characteristic equation is hard to solve in this completely general case. In order to get a start on it, we make some simplifying assumptions. First, suppose that  $K = 1$ , so  $\xi = a/c$ . Next, suppose  $b_1 = b_2 < c$ , and choose  $a = c(\sqrt{c/b_1} - 1)$ , so that  $\beta = b_1$  as well. In this case,  $\phi = b_1a/c$ , and the characteristic equation becomes  $(\lambda + b)^3 + b_1^3a/c = 0$ . The solutions of this characteristic equation are  $\lambda_1 = -b_1(1 + \sqrt[3]{a/c})$ ,  $\lambda_{2,3} = -b_1 + b_1\sqrt[3]{a/c}[\cos(\pi/3) \pm i\sin(\pi/3)]$ . The dynamical system has a Hopf bifurcation when  $\text{Re}(\lambda_{2,3}) = 0$ , i.e., when  $a = 8c$ . Hence, at the Hopf bifurcation,  $c = 81b_1$  and  $a = 8c = 648b_1$ . If we set  $b_1 = 0.2$ , then the Hopf bifurcation occurs at  $c = 16.2$ ,  $a = 129.6$ . At this Hopf bifurcation the period of oscillation is close to  $2\pi/\text{Im}(\lambda_{2,3}) = 2\pi/(b_1\sqrt{3}) = 18$ . Starting at this point, we can trace out the locus of Hopf bifurcations numerically as  $a$  and  $c$  vary at fixed  $b_1$ . See Figure 9.8.

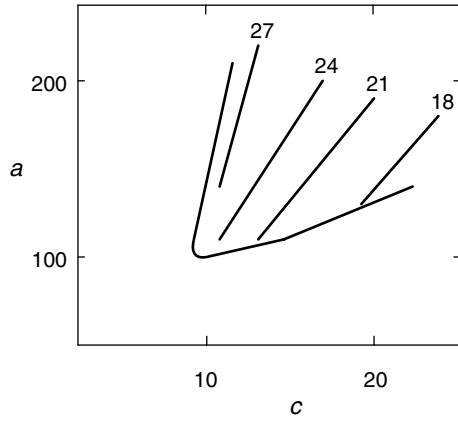


**Figure 9.8** Locus of Hopf bifurcations in the Bliss–Painter–Marr equations given in system (9.18), for  $b_1 = b_2 = 0.2$ . We also plot loci of constant period (18–27) within the region of limit cycle oscillations.

## 9.5 Time-Delayed Negative Feedback

In Goodwin’s equations and Bliss–Painter–Marr’s modified version, we assumed implicitly that there are no time delays in the processes of transcription, translation, or end product repression. However, there are surely some delays in transcription and translation associated with mRNA and protein processing in the nucleus and cytoplasm, respectively. And there are also bound to be delays in the feedback term, because the end product must move into the nucleus, bind with transcription factors, and interact with the “upstream” regulatory sites of the gene to affect its rate of transcription. If we lump all these delays together, we can write a delayed-differential equation for negative feedback:

$$\frac{d[X]}{dt} = \frac{a}{1 + (Z/K_m)^p} - b[X], \quad (9.18)$$

where  $Z(t)$  is a functional of the past history of  $[X](t)$ . For a discrete time lag,

$$Z(t) = [X](t - \tau), \quad (9.19)$$

with  $\tau = \text{constant}$ . For a distributed time lag,

$$Z(t) = \int_{-\infty}^t [X](s) G_c^n(t-s) ds, \quad \text{with } G_c^n(s) = \frac{c^{n+1}}{n!} s^n e^{-cs}. \quad (9.20)$$

The kernel  $G_c^n(s)$  is plotted in Figure 9.9. In Exercise 11 you are asked to show that  $G_c^n$  has a maximum at  $s = n/c$ . As  $n$  and  $c$  increase, with  $n/c$  fixed, the kernel approaches a delta function, and the distributed time lag approaches the discrete time lag with  $\tau = n/c$ . In the same exercise, you are asked to prove that  $d/ds(G_c^n(s)) = c[G_c^{n-1}(s) - G_c^n(s)]$ , a fact that we shall presently put to good use.

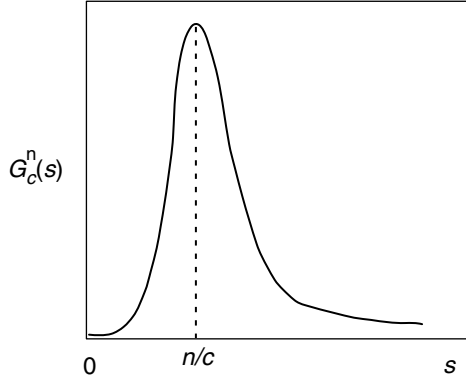


**Figure 9.9** The shape of the kernel  $G_c^n(s)$  for distributed time lag in (9.20).

### 9.5.1 Distributed Time Lag and the Linear Chain Trick

Let us introduce a family of  $Z_j$ 's,

$$Z_j(t) = \int_{-\infty}^t [\mathbf{X}](s) G_c^j(t-s) ds, \quad j = 0, 1, \dots, n.$$

Notice that  $Z_n(t)$  is just the functional  $Z(t)$  in (9.20). Differentiating the definite integral, we find that

$$\frac{dZ_j}{dt} = [\mathbf{X}](t) G_c^j(0) + \int_{-\infty}^t [\mathbf{X}](s) \frac{d}{dt} G_c^j(t-s) ds, \quad j = 0, 1, \dots, n.$$

Since  $G_c^0(0) = c$  and  $G_c^j(0) = 0$  for  $j = 1, \dots, n$ , we see that

$$\begin{aligned} \frac{dZ_0}{dt} &= c[\mathbf{X}](t) + \int_{-\infty}^t [\mathbf{X}](s) [-cG_c^0(t-s)] ds, \\ \frac{dZ_j}{dt} &= \int_{-\infty}^t [\mathbf{X}](s) [cG_c^{j-1}(t-s) - cG_c^j(t-s)] ds, \quad j = 1, \dots, n. \end{aligned}$$

Hence, (9.18) with  $Z$  defined in (9.20) can be written equivalently as a set of ODEs:

$$\begin{aligned} \frac{d[\mathbf{X}]}{dt} &= \frac{a}{1 + (Z_n/K_m)^p} - b[\mathbf{X}], \\ \frac{dZ_0}{dt} &= c([\mathbf{X}] - Z_0), \\ \frac{dZ_j}{dt} &= c(Z_{j-1} - Z_j), \quad j = 1, 2, \dots, n. \end{aligned}$$

That is, the distributed time-delay model, with kernel  $G_c^n(s)$ , is identical to a Goodwin negative feedback loop of length  $n + 2$ . To see this, scale  $[\mathbf{X}], Z_0, \dots, Z_n$  by  $K_m$

and  $t$  by  $K_m/a$  to put these equations into the classical, dimensionless form of Goodwin's equations, (9.18). For simplicity, let  $c = b$ . Then, according to the results of Exercise 8, the loop has a Hopf bifurcation at  $(bK_m/a) = (p - p_{\min})/(\xi p)$ , where  $p_{\min} = [\sec(\pi/(n+2))]^{n+2}$  and the dimensionless number  $\xi$  is the unique real positive root of  $\xi^{p+1} + \xi - a/(bK_m) = 0$ .

As an example, suppose  $n = 6$  and  $p = 4$ . In this case,  $p_{\min} = 1.884$  and the Hopf bifurcation occurs at  $0.529 = (bK_m/a)\xi = 1/(1 + \xi^4)$ , or  $\xi = 0.9714$ . Hence, the critical value of  $b$  is  $b_{\text{crit}} = 0.5446a/K_m$ , and oscillations occur for  $b < b_{\text{crit}}$ . The period of oscillation close to the Hopf bifurcation is  $2\pi/(b_{\text{crit}}\sqrt{3}) \approx 6.66K_m/a$ .

## 9.5.2 Discrete Time Lag

For the case of a discrete time lag, we must solve the delay-differential equation

$$\frac{dx}{dt} = \frac{1}{1 + x(t - \tau)^p} - bx, \quad (9.21)$$

where  $x$  and  $t$  have been scaled to eliminate the parameters  $a$  and  $K_m$  from (9.18). (To do this, let  $x = [X]/K_m$ , dimensionless time  $= at/K_m$ , and dimensionless "b"  $= bK_m/a$ .) Then (9.21) has a steady-state solution  $x^*$  satisfying  $x^{p+1} + x - b^{-1} = 0$ . To investigate the stability of the steady state, we use Taylor's theorem to expand (9.21) in terms of small deviations from the steady state,  $y(t) = x(t) - x^*$ ,

$$\begin{aligned} \frac{dy}{dt} &= -\phi y(t - \tau) - by(t) + \text{higher-order terms}, \\ \phi &= \frac{p(x^*)^{p-1}}{(1 + (x^*)^p)^2} = pb(1 - bx^*) = \frac{pb}{1 + (x^*)^{-p}}. \end{aligned}$$

Looking for solutions of the form  $y(t) = y_0 e^{\lambda t}$ , we find that  $\lambda$  must satisfy the characteristic equation  $\lambda + b = -\phi e^{-\lambda\tau}$ . At a Hopf bifurcation, the eigenvalue  $\lambda$  must be purely imaginary;  $\lambda = \pm i\omega$ . Thus, for (9.21) to exhibit periodic solutions at a Hopf bifurcation, we must insist that

$$b = -\phi \cos(\omega\tau), \quad \omega = \phi \sin(\omega\tau). \quad (9.22)$$

From these equations we can determine the oscillatory frequency ( $\omega$ ) and critical time delay ( $\tau_{\text{crit}}$ ) at the onset of limit cycle oscillations:

$$\begin{aligned} \omega &= \sqrt{\phi^2 - b^2} = b\sqrt{[p/(1 + (x^*)^{-p})]^2 - 1}, \\ \tau_{\text{crit}} &= \frac{\cos^{-1}(-[1 + (x^*)^{-p}]/p)}{b\sqrt{[p/(1 + (x^*)^{-p})]^2 - 1}}. \end{aligned} \quad (9.23)$$

Because the domain of  $\cos^{-1}$  is  $[-1, 1]$ , a necessary condition for Hopf bifurcation is  $1 + (x^*)^{-p} < p$ . For example, if  $p = 4$ , then  $x^*$  must be  $> (1/3)^{1/4} \approx 0.760$ , which implies that  $b = (x^{p+1} + x)^{-1} < 3^{5/4}/4 \approx 0.987$ . If  $b = 1/2$ , then  $x^* = 1$  and  $\omega = \sqrt{3}/2$ . Because  $\cos(\omega\tau) = -b/\phi = -1/2$ ,  $\tau = 4\pi\sqrt{3}/9$ . Hence, for  $b = 1/2$  and  $p = 4$ , small-amplitude

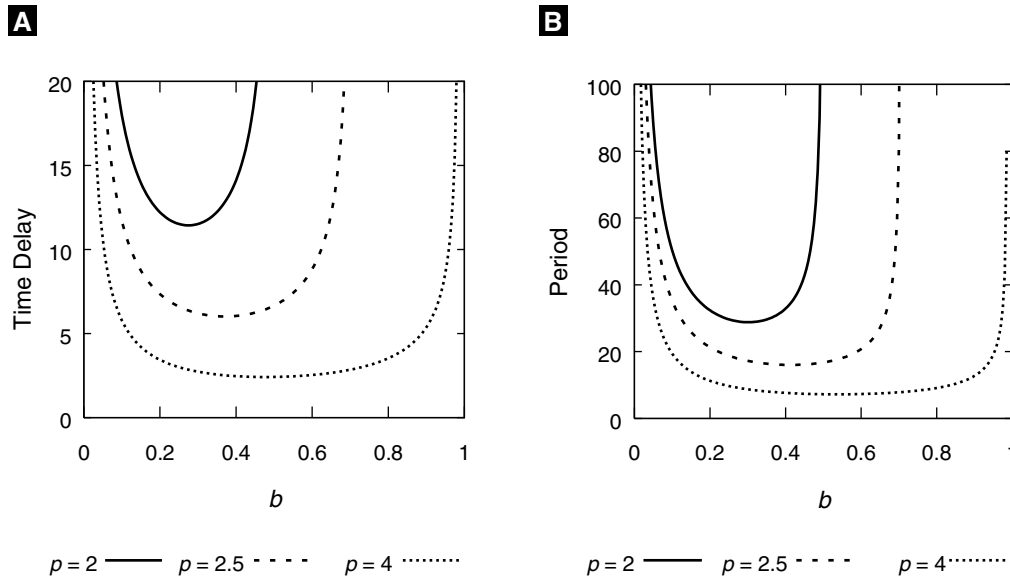


**Figure 9.10** Loci of Hopf bifurcations in (9.21). We plot  $\tau_{\text{crit}}$  and period ( $2\pi/\omega$ ) as functions of  $b$ , for three values of  $p$ : 2 (solid line), 2.5 (dashed line), and 4 (dotted line). Oscillatory solutions lie within the U-shaped domains. Notice that for  $p = 4$ ,  $b = 0.5$ , as calculated in the text,  $\tau_{\text{crit}} = 2.418$  and period = 7.255.

oscillations, with period =  $2\pi/\omega \approx 7.255$ , bifurcate from the steady state as the time delay increases beyond 2.418. In Figure 9.10 we show how the characteristics of these Hopf bifurcations ( $\tau_{\text{crit}}$  and period) depend on  $b$ , for fixed values of  $p$ .

## 9.6 Circadian Rhythms

Everyone is familiar with his or her own 24-hour sleep–wake cycle. Many other aspects of human physiology also exhibit daily rhythms, including body temperature, urine production, hormone secretion, and skin cell division. Such rhythms are observed in all kinds of plants, animals, and fungi, as well as unicellular organisms, and even cyanobacteria. Because these rhythms persist in the absence of external cues (light intensity, temperature, etc.), they reflect an endogenous oscillator within cells that runs at a period close to 24 h.

Biologists have long been puzzled by the molecular basis of circadian rhythms. Although a fundamental breakthrough was made by Konopka and Benzer in 1971 (Konopka and Benzer 1971), with their discovery of the *per* gene in *Drosophila* (mutations of which alter the endogenous circadian rhythm of affected flies), it was 25 years before the molecular details of the circadian oscillator began to become clear. We know now that PER protein inhibits transcription of the *per* gene, through a complicated pro-

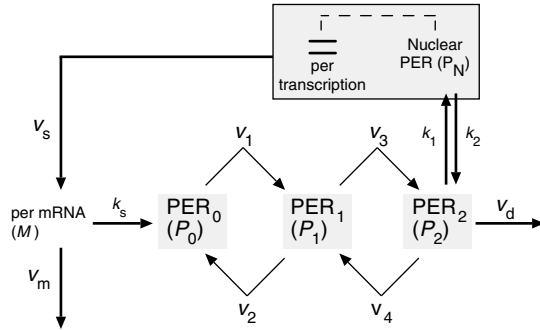


**Figure 9.11** Goldbeter's model of circadian rhythms (Goldbeter 1995). PER protein is synthesized in the cytoplasm, where it is successively phosphorylated, as indicated by subscripts. The doubly phosphorylated form enters the nucleus and represses transcription of the *per* gene.

cess involving phosphorylation by DBT kinase, binding to TIM subunits, transport into the nucleus, and interaction with the transcription factors (CLK and CYC).

It is clear to all that the control system is dominated by a time-delayed negative-feedback loop, quite close in principle to Goodwin's original negative feedback oscillator. Numerous theoreticians have exploited the interesting nonlinear dynamics of delayed negative feedback in order to model certain characteristics of circadian rhythms. Ruoff and Rensing have explored the capabilities of Goodwin's Equation (9.18), with  $p = 9$ , to account for temperature compensation, entrainment, and phase resetting (Ruoff and Rensing 1996).

Goldbeter proposed a more complicated model, based loosely on Goodwin's idea, supplemented with reversible phosphorylation steps and nuclear transport; see Figure 9.11 (Goldbeter 1995). The kinetic equations describing this mechanism are

$$\begin{aligned}\frac{dM}{dt} &= \frac{v_s}{1 + (P_N/K_1)^4} - \frac{v_m M}{K_{m1} + M}, \\ \frac{dP_0}{dt} &= k_s M - \frac{V_1 P_0}{K_1 + P_0} + \frac{V_2 P_1}{K_2 + P_1}, \\ \frac{dP_1}{dt} &= \frac{V_1 P_0}{K_1 + P_0} - \frac{V_2 P_1}{K_2 + P_1} - \frac{V_3 P_1}{K_3 + P_1} + \frac{V_4 P_2}{K_4 + P_2}, \\ \frac{dP_2}{dt} &= \frac{V_3 P_1}{K_3 + P_1} - \frac{V_4 P_2}{K_4 + P_2} - k_1 P_2 + k_2 P_N - \frac{v_d P_2}{K_d + P_2}, \\ \frac{dP_N}{dt} &= k_1 P_2 - k_2 P_N.\end{aligned}$$

The basal parameter values are:

$$\begin{aligned}v_s &= 0.76 \mu\text{M/h}, v_m = 0.65 \mu\text{M/h}, v_d = 0.95 \mu\text{M/h}, \\ k_s &= 0.38 \text{h}^{-1}, k_1 = 1.9 \text{h}^{-1}, k_2 = 1.3 \text{h}^{-1}, \\ V_1 &= 3.2 \mu\text{M/h}, V_2 = 1.58 \mu\text{M/h}, V_3 = 5 \mu\text{M/h}, V_4 = 2.5 \mu\text{M/h}, \\ K_1 &= K_2 = K_3 = K_4 = 2 \mu\text{M}, K_1 = 1 \mu\text{M}, K_{m1} = 0.5 \mu\text{M}, K_d = 0.2 \mu\text{M}.\end{aligned}$$

Figure 9.12A shows a numerical simulation of this system of ODEs, with a period close to 24 h. Figure 9.12B shows how the period of oscillation depends on  $v_d$ , the

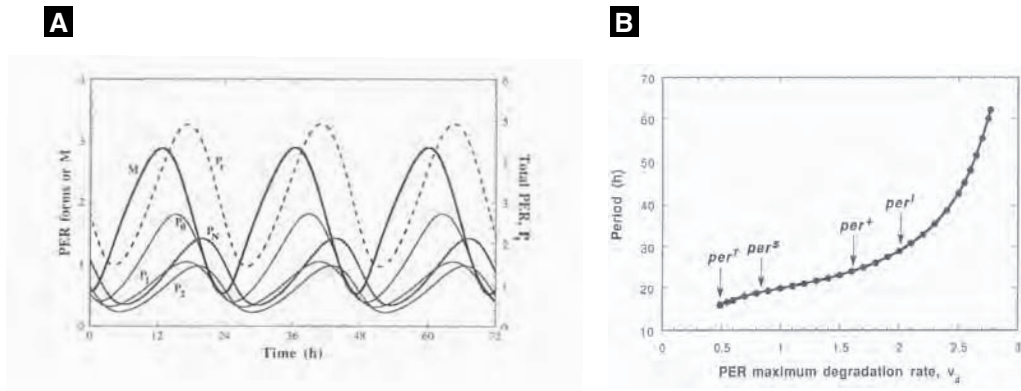


**Figure 9.12** Simulations of Goldbeter's model. (A) mRNA and protein concentrations as functions of time. (B) Period of oscillation as a function of  $v_d$ . Figures are reprinted from Goldbeter (1995).

degradation rate of PER. Goldbeter suggested that the short-period mutant of *per* (*per<sup>S</sup>* has an autonomous period of 19 h) encodes a more stable form of PER, and the long-period mutant (*per<sup>L</sup>* has an autonomous period of 28 h) encodes a less stable form of PER (Goldbeter 1995). In subsequent papers, Leloup and Goldbeter have studied temperature compensation and phase resetting in this model (Leloup and Goldbeter 1998; Leloup and Goldbeter 1999).

Perhaps the simplest model of circadian rhythms is negative feedback with discrete time delay described by (9.18) and (9.19), which has been explored in a recent paper by Lema, Golombek, and Echave (Lema et al. 2000). In this case, X is PER,  $a$  = maximum rate of PER synthesis,  $b$  = rate constant for PER degradation,  $K_m$  = PER concentration at half-maximal synthesis rate, and  $\tau$  = time delay (because the rate of synthesis of PER at the present moment depends on its cytoplasmic concentration some time in the past). (Lema et al. chose  $a = 1 \text{ h}^{-1}$ ,  $b = 0.4 \text{ h}^{-1}$ ,  $K_m = 0.04$ ,  $\tau = 8 \text{ h}$ , and  $p = 2.5$ .) In Section 9.5.2 we showed how to do stability analysis of the steady state of this delay-differential equation, in order to find the points of Hopf bifurcation to periodic solutions. Letting  $x^*$  be the unique real positive root of  $x^{p+1} + x - [a/(bK_m)] = 0$ , we find that periodic solutions exist for  $\tau > (K_m/a)\tau_{\text{crit}}$ , with  $\tau_{\text{crit}}$  (dimensionless) given by (9.23). The period of oscillation of the bifurcating solutions is close to  $2\pi/\omega$ , where  $\omega\tau = \cos^{-1}(-[1 + (x^*)^{-p}]/p)$ . For the parameter values chosen by Lema et al.,  $a/(bK_m) = 62.5$ ,  $x^* = 3.21$ ,  $\omega = 0.0344$ , and  $\tau_{\text{crit}} = 58.1$ . Hence, for  $\tau > 2.33 \text{ h}$ , their model oscillates with period close to  $2\pi/\omega \approx \pi\tau \approx 7.32 \text{ h}$ . To get a period close to 24 h, they chose  $\tau = 8 \text{ h}$ . In their paper Lema et al. explored entrainment by phase-resetting in response to light pulses, assuming that light interacts with PER dynamics at either the synthesis ( $a$ ) or degradation ( $b$ ) step.

Tyson and coworkers have taken a different approach, noting that phosphorylation of PER by DBT induces rapid degradation of PER, but multimers of PER and TIM are

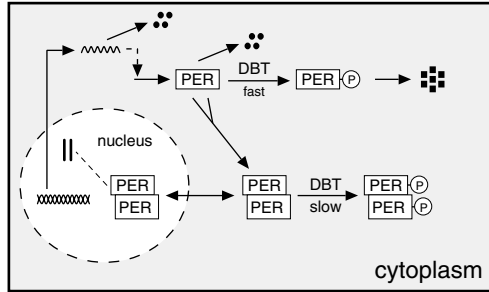


**Figure 9.13** An alternative model of circadian rhythms (Tyson et al. 1999). The circadian protein PER is synthesized in the cytoplasm, where it can form homodimers, PER:PER. (Multimeric protein complexes with TIM are neglected in this simple model.) PER monomers are rapidly phosphorylated by a protein kinase called DBT, and phosphorylated PER is rapidly degraded. PER dimers are only slowly phosphorylated by DBT.

not readily phosphorylated by DBT; see Figure 9.13 (Tyson et al. 1999). They describe this mechanism by three ODEs

$$\begin{aligned}\frac{dM}{dt} &= \frac{v_m}{1 + (P_2/A)^2} - k_m M, \\ \frac{dP_1}{dt} &= v_p M - \frac{k_1 P_1}{J + P_1 + 2P_2} - k_3 P_1 - 2k_a P_1^2 + 2k_d P_2 + \frac{2k_2 P_2}{J + P_1 + 2P_2} + 2k_3 P_2, \\ \frac{dP_2}{dt} &= k_a P_1^2 - k_d P_2 - \frac{2k_2 P_2}{J + P_1 + 2P_2} - 2k_3 P_2,\end{aligned}$$

where

$M = [\text{per mRNA}]$ ,  $P_1 = [\text{PER monomer}]$ ,  $P_2 = [\text{PER dimer}]$ ,  
 $v_m, v_p =$  rate constants for synthesis of mRNA and protein,  
 $k_m, k_3 =$  rate constants for non-specific degradation of mRNA and protein,  
 $k_1, k_2 =$  rate constants for phosphorylation of monomer and dimer  
 $k_a, k_d =$  rate constants for association and dissociation of dimer,  
 $J, A =$  Michaelis constants for the binding of PER to phosphatase and transcriptional regulation factors.

If the dimerization reaction is in rapid equilibrium, then  $P_1 = qP_T$  and  $P_2 = ((1 - q)/2)P_T$ , where  $P_T = P_1 + 2P_2 = [\text{total protein}]$ , and

$$q = \frac{2}{1 + \sqrt{1 + 8KP_T}},$$

where  $K = k_a/k_d =$  the equilibrium binding constant for dimer formation. In this case, the system of three ODEs reduces to a pair of ODEs:

$$\begin{aligned}\frac{dM}{dt} &= \frac{v_m}{1 + (P_2/A)^2} - k_m M, \\ \frac{dP_T}{dt} &= v_p M - \frac{k_1 P_1 + 2k_2 P_2}{J + P_T} - k_3 P_T,\end{aligned}$$

with  $P_1$  and  $P_2$  given as functions of  $P_T$  by the equations above. Figure 9.14A shows a phase plane portrait for this system, with limit cycle oscillations of period close to 24 h. Figure 9.14B shows how these oscillations depend on  $k_1$ , the rate constant for



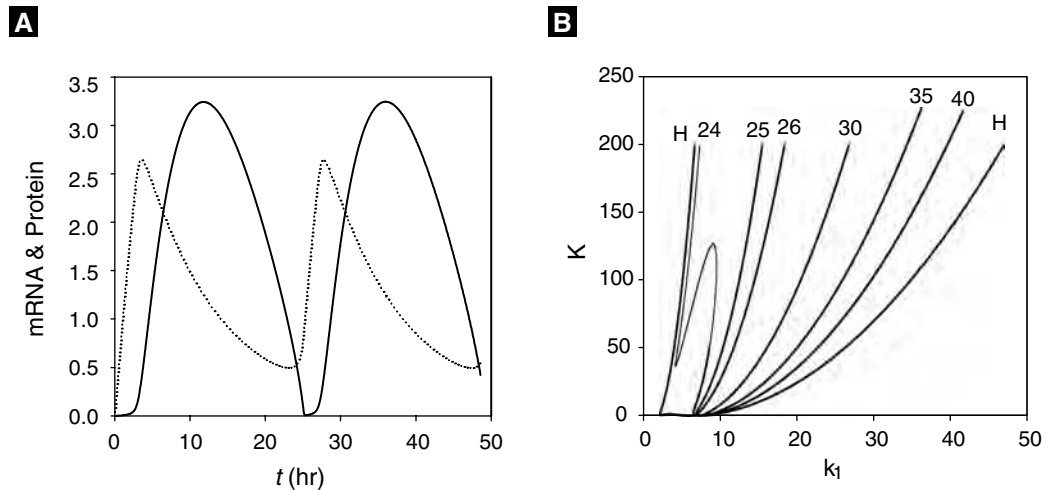


**Figure 9.14** Simulations of the model of Tyson et al. (1999). Basal parameter values:  $v_m = 1$ ,  $v_p = 0.5$ ,  $k_m = k_3 = 0.1$ ,  $k_1 = 10$ ,  $k_2 = 0.03$ ,  $J = 0.05$ ,  $K = 200$ ,  $A = 0.1$  (A) mRNA and protein concentrations as functions of time. (B) Locus of Hopf bifurcations (H) in dependence on  $k_1$  and  $K$ . Also indicated are loci of limit cycles of constant period (24 h, 25 h, ..., 40 h).

phosphorylation of PER monomers by DBT, and  $K$ , the equilibrium binding constant for dimer formation.

## Suggestions for Further Reading

- Joseph Higgins published the first comprehensive theory of biochemical oscillators, and it is still valuable reading today (Higgins 1967).
- The earliest collection of articles on biological and biochemical oscillators was edited by Chance, Pye, Ghosh, and Hess, B. (Chance et al. 1973).
- For a comparative survey of cellular oscillators see (Berridge and Rapp 1979).
- Sol Rubinow's 1980 chapter is one of the best summaries of the kinetics of regulatory enzymes (Rubinow 1980).
- Although not easy reading, Albert Goldbeter's 1996 book *Biochemical Oscillators and Cellular Rhythms* is comprehensive, authoritative, and well motivated (Goldbeter 1996).

**Acknowledgment:** JJT thanks Emery Conrad for help in writing this chapter.

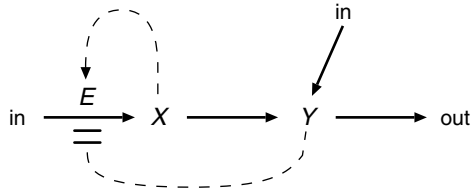


Figure 9.15 Exercise 1

## 9.7 EXERCISES

1. Activator–inhibitor system. Consider the mechanism in Figure 9.15, which can be described by the (scaled) differential equations

$$\frac{dx}{dt} = \frac{a + bx^2}{1 + x^2 + ry} - x,$$

$$\frac{dy}{dt} = \epsilon(cx + y_0 - y).$$

Basal parameter values:  $a = 1$ ,  $b = 5$ ,  $c = 4$ ,  $r = 1$ ,  $y_0 = 0$ ,  $\epsilon = 0.1$ .

- (a) Why is this called an activator–inhibitor system?
  - (b) Draw a phase plane portrait (nullclines and typical trajectories) for the basal parameter values.
  - (c) Vary  $c$  and find the Hopf bifurcation points.
  - (d) As you vary both  $c$  and  $y_0$ , how many qualitatively different phase plane portraits can you find? Sketch them.
2. Substrate–depletion system. Consider the mechanism in Figure 9.16, which can be described by the (scaled) differential equations

$$\frac{dx}{dt} = a - xy^2, \quad \frac{dy}{dt} = \epsilon + xy^2 - by$$

Basal parameter values:  $a = 0.5$ ,  $b = 1$ ,  $\epsilon = 0.05$

- (a) Why is this called a substrate–depletion system?
  - (b) Rewrite the ODEs in terms of  $y$  and  $z = x + y$ .
  - (c) Draw a phase plane portrait (nullclines and typical trajectories) for the basal parameter values.
  - (d) Classify the stability of the steady state as  $a$  varies.
3. Substrate–inhibition oscillator (Murray 1981). Perhaps the simplest example of a biochemical oscillator is illustrated in Figure 9.17. The rate equations for this mechanism

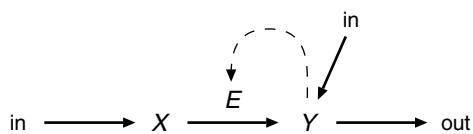


Figure 9.16 Exercise 2

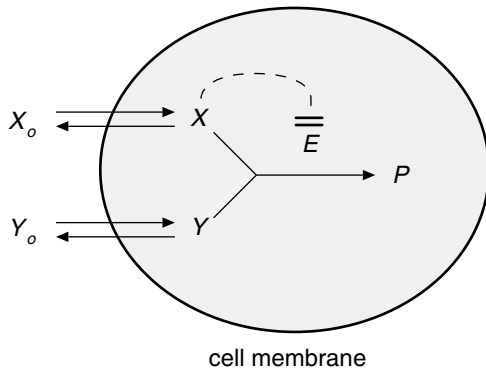


Figure 9.17 Exercise 3

are

$$\frac{dX}{dt} = a(X_0 - X) - \frac{\nu XY}{K_{m1} + X + (X^2/K_{m2})},$$

$$\frac{dY}{dt} = b(Y_0 - Y) - \frac{\nu XY}{K_{m1} + X + (X^2/K_{m2})},$$

where  $a, b$  are membrane permeabilities,  $\nu$  is a rate constant, and the  $K_m$ 's are dissociation constants of the enzyme-substrate complexes. Basal parameter values:  $a = 1, b = 0.15, X_0 = 1, Y_0 = 6, \nu = 30, K_{m1} = 1, K_{m2} = 0.005$ .

- Plot nullclines and some characteristic trajectories.
  - Find points of Hopf bifurcation as  $Y_0$  varies.
  - For  $b = 1, X_0 = 1.5, Y_0 = 4$ , plot nullclines and trajectories.
  - For  $b = 1$ , find the region of bistability in the  $(X_0, Y_0)$  plane.
4. Gene expression (Keller 1995). Consider a bacterial operon expressing two genes, *genX* and *genY*, as in Figure 9.18. The proteins  $X$  and  $Y$  form homodimers  $X_2$  and  $Y_2$ , which then bind to the upstream regulatory sequence and affect the expression of *genX* and *genY*.  $X_2$ -binding stimulates gene expression, but  $Y_2$ -binding inhibits it. Assume that the homodimers are very stable and that they bind to the regulatory sequence with equal affinity.

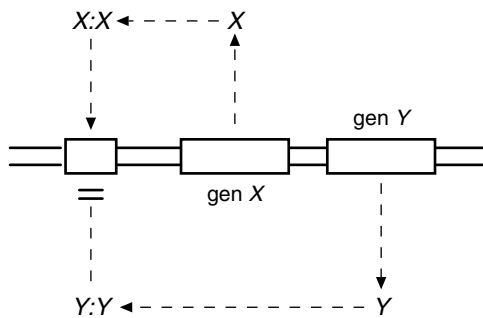


Figure 9.18 Exercise 4

(a) Show that the mechanism can be described by a pair of (scaled) ODEs,

$$\frac{dx}{dt} = 1 + \frac{\alpha x^2}{1+x^2+y^2} - \beta x, \quad \frac{dy}{dt} = \epsilon \left( 1 + \frac{\alpha x^2}{1+x^2+y^2} \right) - \gamma y,$$

where  $\epsilon$  is the rate of expression of Y relative to that of X.

(b) Construct a phase plane portrait for this system when  $\alpha = 50, \beta = 10, \gamma = 1, \epsilon = 0.2$ .

(c) Would you describe this oscillator as activator-inhibitor or substrate-depletion?

(d) Find the locus of Hopf bifurcations in the  $(\beta, \gamma)$  parameter plane.

5. Glycolysis. In Section 9.3.1 we studied a simple model of the glycolytic oscillator, system (9.12), and found that oscillations exist within a limited range of substrate injection rates,  $k_{1lo} < k_1 < k_{1hi}$ , where  $k_{1lo} = \epsilon k_3 K_n$ , and  $k_{1hi} = (k_3 K_n) / (\sqrt{1 + \nu})$ , with  $\nu = \nu_2 / k_3$  (See (9.16)).

(a) Show that the period of oscillation close to the two Hopf bifurcation points is given by

$$T_{lo} = \frac{2\pi}{k_3 \epsilon \sqrt{2\nu}}, \quad T_{hi} = \frac{2\pi}{k_3} \sqrt{\frac{2 + \nu}{\nu}}.$$

(b) Hess and Boiteux (Chance et al. 1973) reported that  $k_{1lo} = 0.33$  mM/min,  $T_{lo} = 8.6$  min, and  $k_{1hi} = 2.5$  mM/min,  $T_{hi} = 3.5$  min. Supposing that  $\nu \ll 1$ , show that  $\epsilon \cong k_{1lo} / k_{1hi} = 0.13$  and  $T_{hi} / T_{lo} \cong 2\epsilon \cong 0.25$ , which is not too far from the observed ratio 0.4.

(c) For the parameter values  $\epsilon^2 = 0.017, K_n = 0.25$  mM,  $\nu_2 = 1$  min<sup>-1</sup> and  $k_3 = 10$  min<sup>-1</sup>, use a numerical bifurcation package to compute  $k_{lo}, T_{lo}, k_{1hi}$ , and  $T_{hi}$ , and compare your results to the observations of Hess and Boiteux.

6. Positive feedback on gene transcription (Griffith 1968b). Consider the simple case of a protein that activates transcription of its own gene, as in Figure 9.19. This mechanism is described by a pair of ODEs:

$$\frac{d[M]}{dt} = v_1 \frac{\epsilon^2 + ([P]/K_t)^2}{1 + ([P]/K_t)^2} - k_2[M], \quad \frac{d[P]}{dt} = k_3[M] - k_4[P].$$

(a) How must the variables be scaled to write the ODEs in dimensionless form:

$$\frac{dx}{d\tau} = \frac{\epsilon^2 + y^2}{1 + y^2} - x, \quad \frac{dy}{d\tau} = \kappa(\sigma x - y)?$$

(b) Assume that  $\epsilon = 0.2, \kappa = 1$ , and draw phase plane portraits for several values of  $\sigma$ .

(c) Find the bifurcation values of  $\sigma$ .

(d) Plot  $y$  (the steady-state concentration of P) as a function of  $\sigma$ .

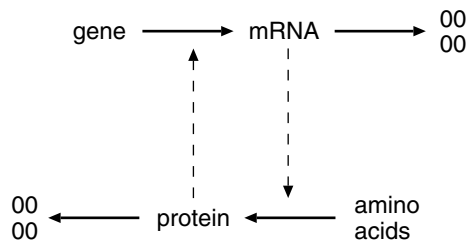


Figure 9.19 Exercise 6

7. Generalize the positive feedback system in the previous problem to a loop of arbitrary length.

- (a) Show that, when properly scaled, the steady state solution of the dynamical equations is given by the roots of

$$\phi z = \frac{\epsilon^p + z^p}{1 + z^p}, \quad (*)$$

where  $\phi = \text{constant}$ ,  $p = \text{an arbitrary exponent}$ , and  $z = \text{the scaled concentration of end product}$ .

- (b) Show that the system has saddle-node bifurcation points when (\*) is satisfied simultaneously with

$$\phi = \frac{pz^{p-1}(1 - \epsilon^p)}{(1 + z^p)^2}. \quad (**)$$

- (c) For  $\epsilon \ll 1$ , show that (\*) and (\*\*) are satisfied simultaneously for

$$z \approx (p - 1)^{1/p},$$

$$\phi \approx p^{-1}(p - 1)^{(p-1)/p},$$

and

$$z \approx \epsilon(p - 1)^{-1/p},$$

$$\phi \approx p\epsilon^{p-1}(p - 1)^{-(p-1)/p}.$$

- (d) Compute the saddle-node bifurcation points for  $p = 2, 3, 4$ , and compare to numerical results (pick some small value of  $\epsilon$ ).

8. Goodwin's equations. Generalize the analysis in Section 9.4.3 to a negative-feedback loop with  $n$  components,

$$\frac{dx_1}{dt'} = \frac{1}{1 + x_n^p} - b_1 x_1, \quad \frac{dx_j}{dt'} = b_j(x_{j-1} - x_j), \quad j = 2, 3, \dots, n.$$

Assume that  $b_1 = b_2 = \dots = b_n = b$ , and show that the steady state ( $x_1 = x_2 = \dots = x_n = \xi$ ) is unstable when  $b\xi < (p - p_{\min})/p$ , where  $p_{\min} = \sec^n(\pi/n)$ . Compute  $p_{\min}$  for  $n = 4, 8, 16$ .

9. Modify the Bliss-Painter-Marr equations given in Section 9.4.3 by replacing  $a/(1 + x_3)$  with  $a/(1 + x_3^p)$  in the first differential equation. Let  $a = 1, b_1 = b_2 = 0.1, K = 1$ . Plot the locus of Hopf bifurcation points in the  $(p, c)$  parameter plane, for  $0 < p < 10$ .

10. Calcium-induced calcium release (Goldbeter et al. 1990). Consider a two-variable model for  $\text{Ca}^{2+}$  oscillations in cells:

$$\frac{dX}{dt} = v_0 + v_1\beta - V_2 + V_3 - k_4X + k_5Y,$$

$$\frac{dY}{dt} = V_2 - V_3 - k_5Y,$$

where

$$V_2 = v_2 \frac{X^2}{K_R^2 + X^2},$$

$$V_3 = v_3 \frac{Y^2}{K_R^2 + Y^2} \cdot \frac{X^4}{K_A^4 + X^4}.$$

In these equations  $X = [\text{Ca}^{2+}]_{\text{cytosolic}}$ ,  $Y = [\text{Ca}^{2+}]_{\text{vesicular}}$ ,

$v_0 = \text{slow leak of } \text{Ca}^{2+} \text{ into the cytosol from extracellular fluid}$ ,

$v_1\beta$  = IP<sub>3</sub>-induced release of Ca<sup>2+</sup> into the cytosol from intracellular stores,

$V_2$  = ATP-dependent Ca<sup>2+</sup> pump,

$V_3$  = Ca<sup>2+</sup>-induced Ca<sup>2+</sup> release from storage vesicles,

$k_4$  = Ca<sup>2+</sup> elimination through the plasma membrane,

$k_5$  = Ca<sup>2+</sup> leak from storage vesicles.

Goldbeter et al. estimated the parameters to be

$$v_0 = 1 \mu\text{M/s}, v_1 = 7.3 \mu\text{M/s}, \beta = 0, v_2 = 65 \mu\text{M/s}, K_2 = 1 \mu\text{M}, \\ v_3 = 500 \mu\text{M/s}, K_R = 2 \mu\text{M}, K_A = 0.9 \mu\text{M}, k_4 = 10 \text{ s}^{-1}, k_5 = 1 \text{ s}^{-1}$$

- Draw a wiring diagram that corresponds to these equations.
  - Draw a phase plane portrait for the basal parameter values.
  - Increase  $\beta$  (the IP<sub>3</sub> signal) from 0 to 1 (its maximum value), and find values that correspond to Hopf bifurcations.
  - To simulate a pulse of IP<sub>3</sub>, let  $\beta(t) = \beta_0 e^{-\alpha t}$ , with  $\alpha = 0.25 \text{ s}^{-1}$ . Try  $\beta_0 = 0.85$  and  $0.95$ . In each case, plot  $X(t)$ .
11. For the distributed time lag defined in (9.20), assume  $n$  is an integer  $\geq 1$  and show that

$$\int_0^{\infty} G_c^n(s) ds = 1$$

(b)

$$\frac{d}{ds} G_c^n(s) = c (G_c^{n-1}(s) - G_c^n(s))$$

(c)

$$G_c^n(s) \text{ has a maximum at } s = n/c.$$

12. Periodic hemolytic anemia (Mackey 1996). Mackey has introduced a time-delayed negative-feedback model of an autoimmune disease that causes periodic crashes in circulating red blood cells (RBC)(see Figure 9.20). When RBC level in the blood is low, the cells produce a hormone, called erythropoietin, that stimulates the production of RBC precursor cells. After a few days, these precursors become mature RBCs and the production of erythropoietin is turned down. Hence, circulating RBC level is controlled by a negative-feedback system with time delay (maturation time). Mackey models this control system with equation (9.21):

$$\frac{dx}{dt} = \frac{1}{1 + x(t - \tau)^p} - bx,$$

where

[X] = concentration of circulating RBCs,

$a$  = maximal rate of production of mature RBCs,

$b$  = loss rate of RBCs from the blood stream,

$K_m$  = RBC concentration when production rate is cut in half,

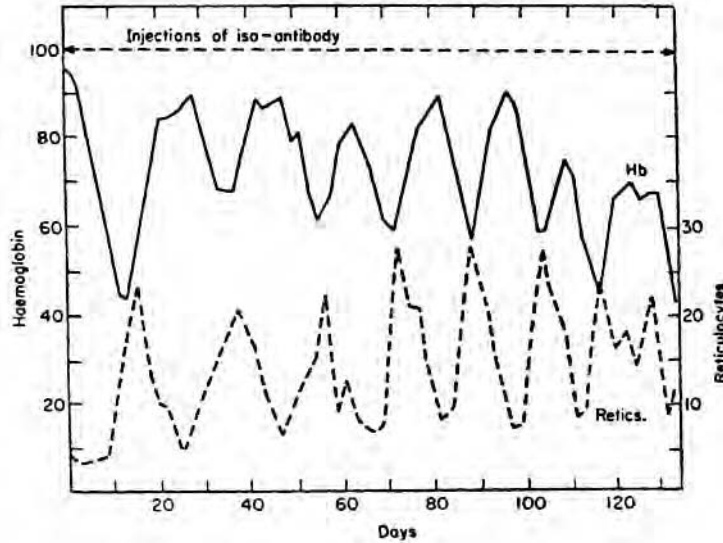


**Figure 9.20** Exercise 12. Laboratory induced autoimmune hemolytic anemia. Oscillations in circulating hemoglobin and reticulocyte counts in rabbit during constant application of red blood cell iso-antibody. From Kirk et al. (1968), as presented in Mackey (1996).

$\tau$  = time required for RBC precursors to develop into mature, circulating RBCs.

The nonlinear term in (9.21) captures the fact that current production of mature RBCs is a decreasing function of RBC concentration in the blood stream  $\tau$  days ago; the parameter  $p$  controls the steepness of this feedback function. Mackey estimated that in normal humans,

$$a = 7.62 \cdot 10^{10} \text{ cell kg}^{-1} \text{ day}^{-1}, \quad b = 2.31 \cdot 10^{-2} \text{ day}^{-1}, \\ K_m = 2.47 \cdot 10^{11} \text{ cell kg}^{-1}, \quad \tau = 5.7 \text{ day}, \quad p = 7.6.$$

- Calculate the steady-state level of circulating RBCs in a normal human, and show that this steady state is stable.
- Periodic hemolytic anemia is an autoimmune disease that can be induced in rabbits by administration of RBC autoantibodies. The immune system destroys RBCs, thereby increasing parameter  $b$  in the model. Treating  $b$  as a bifurcation parameter, show that Mackey's model undergoes a Hopf bifurcation at  $b = 5.12 \cdot 10^{-2}/\text{day}$  and that the resulting oscillation has a period close to 20.6 day. Compare your results to the data in Figure 9.20.
- Show that if  $b$  is elevated beyond 0.27/day, then oscillations are lost by a reverse Hopf bifurcation.
- Plot oscillation period and amplitude ( $[X]_{\max}$  and  $[X]_{\min}$ ) as functions of  $b$  between the two Hopf bifurcations.